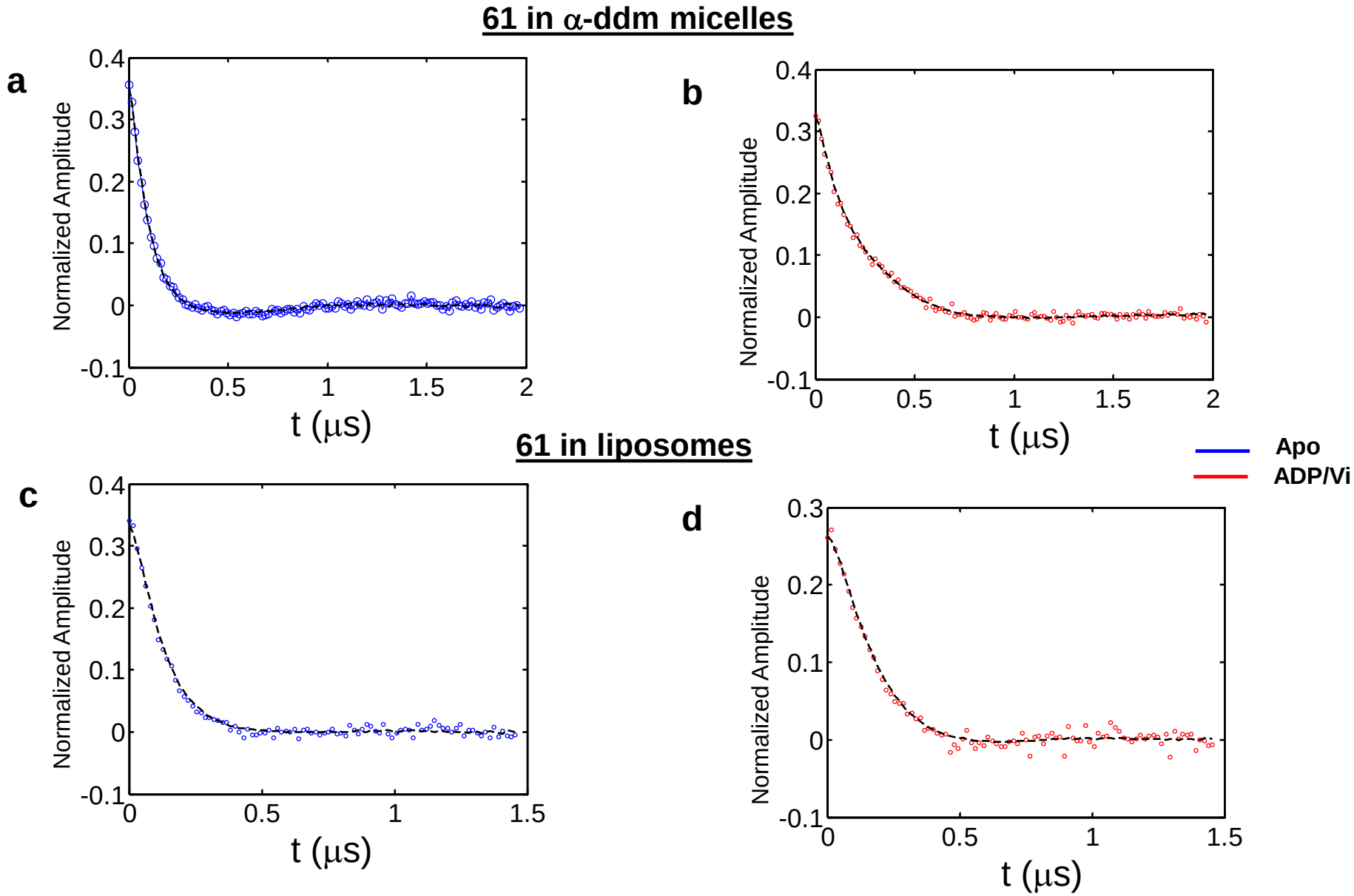

Supplementary Figure S1A (a, c) – Time domain 17.35 GHz DEER signals (after background removal) for MsbA mutant 61 in both liposomes and α-ddm micelles in the apo state are shown along with their fits (dashed lines). (b, d) same as in (a,c) but for the ADP/Vi intermediate.

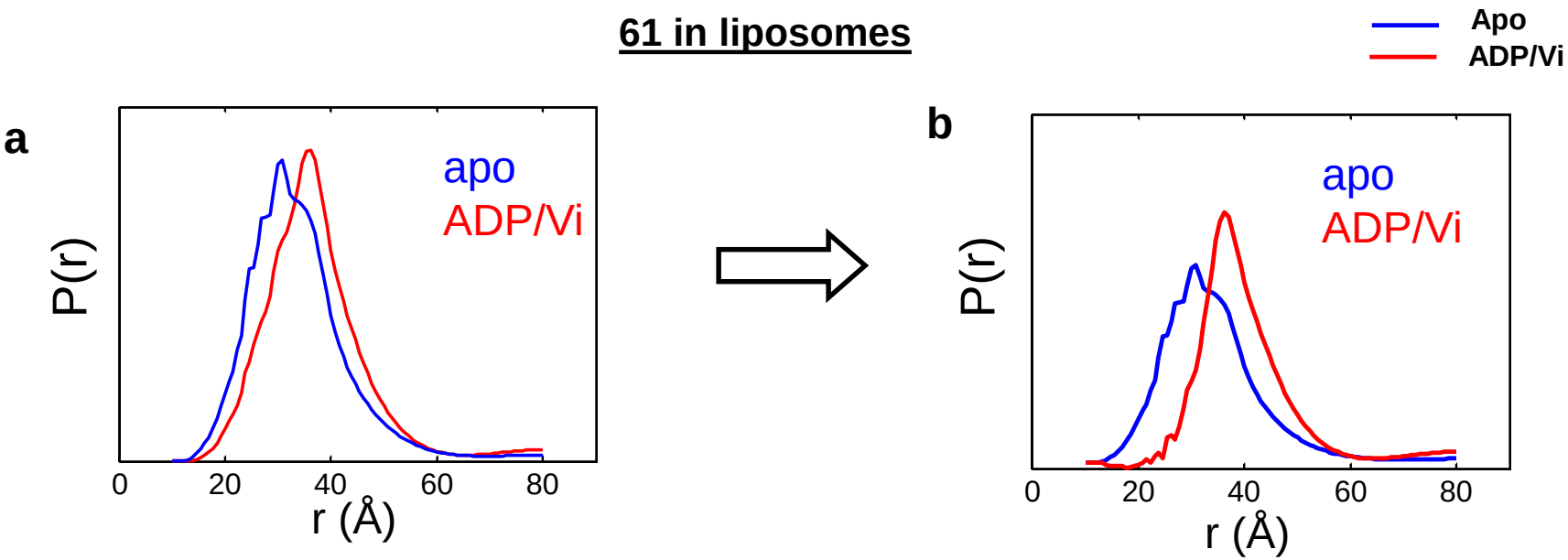

Supplementary Figure S1B. (a) - Distance distributions, P(r), of MsbA mutant 61 in liposomes generated from the time-domain data of Fig. S1A . Note that in the case of liposomes P(r) for ADP/Vi intermediate contains some P(r) for the apo state due to less than 100% conversion from the apo state to the ADP/Vi state. (b) - The P(r) for the ADP/Vi case (in a) after subtracting out a 40% fraction of the apo component; The new component (corresponding to pure ADP/Vi intermediate) and the apo component are plotted individually normalized.

248 in α-ddm micelles

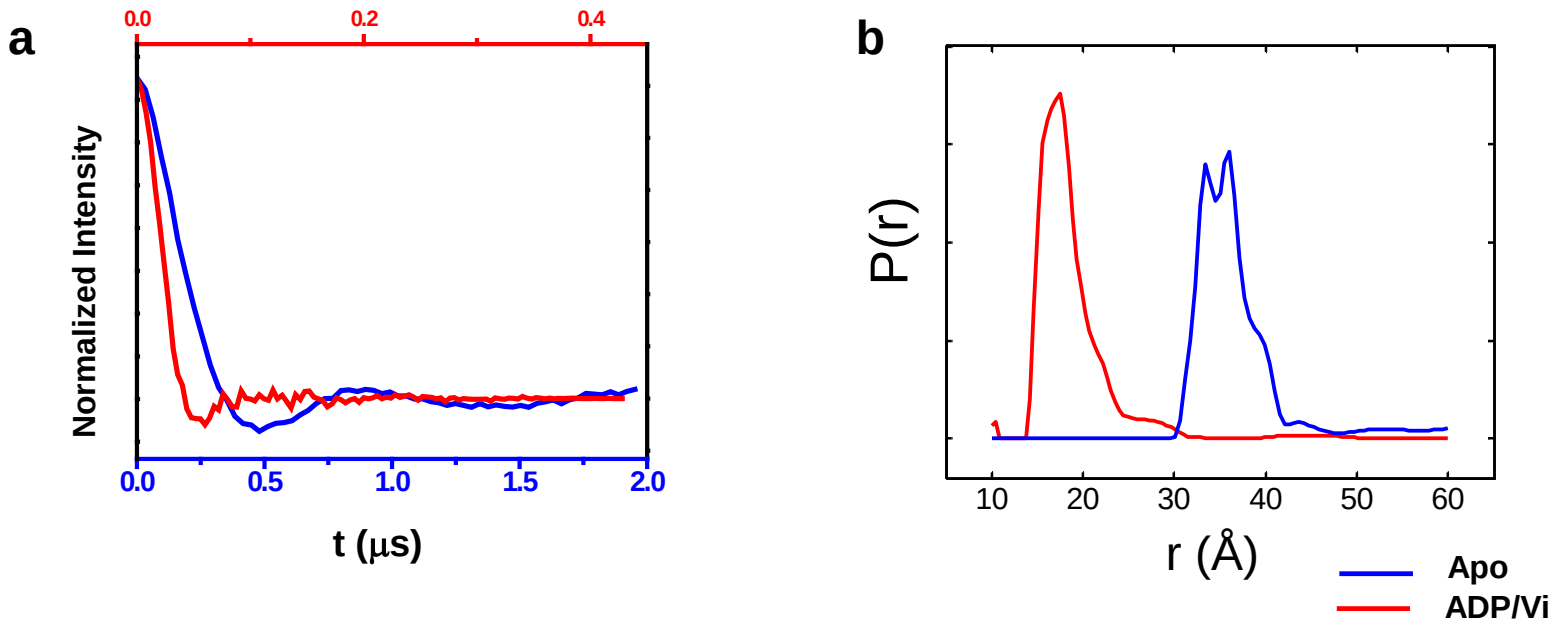

Supplementary Figure S2. (a) - Time domain 17.35 GHz DEER signals (after background removal) for MsbA mutant 248 in α-ddm micelles. (b) - Distance distributions obtained by fitting data from (a) by MEM with background auto-correction.

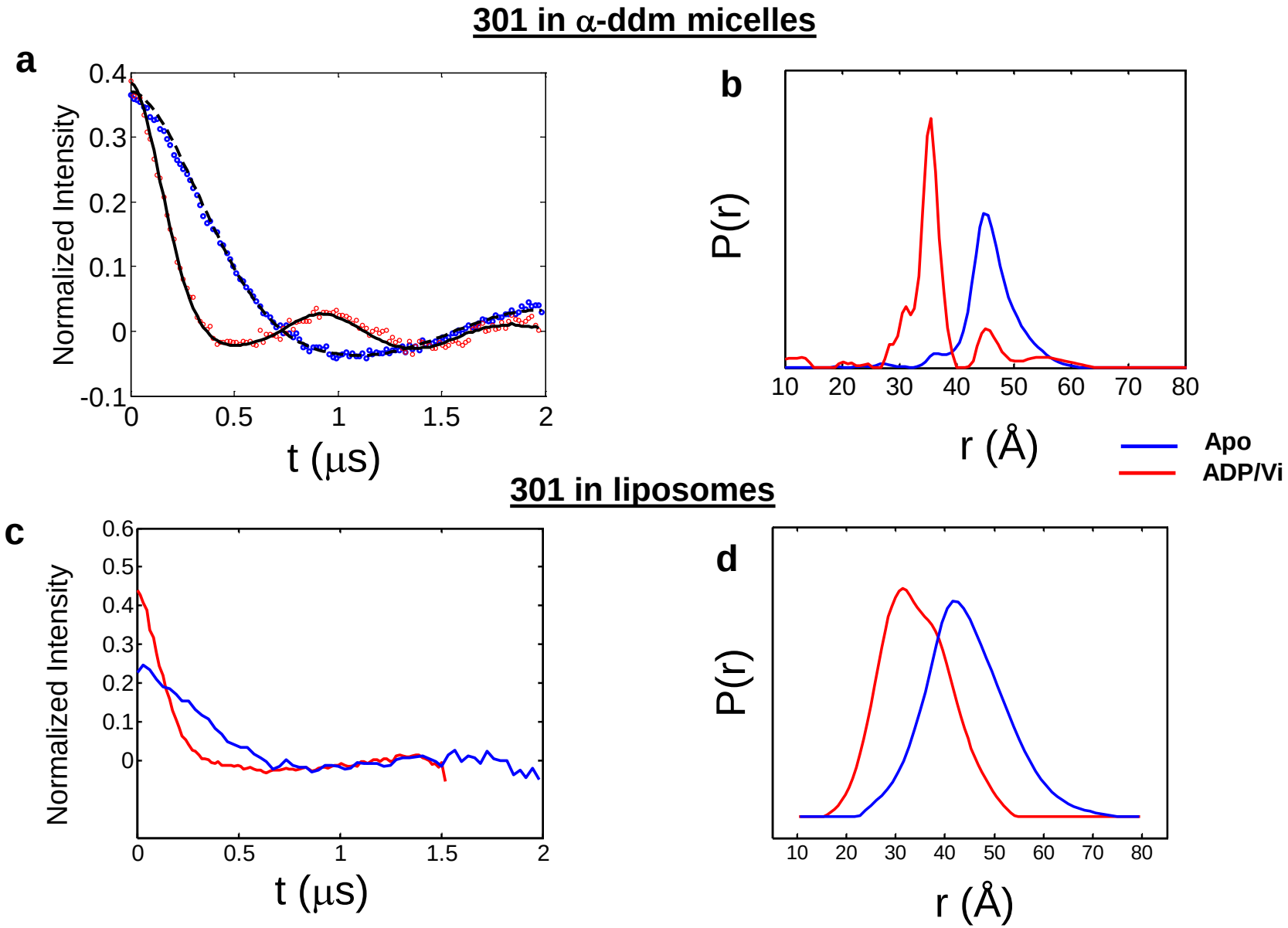

Supplementary Figure S3. (a, c) - Time domain 17.35 GHz DEER signals (after background removal) for MsbA mutant 301 in α-ddm micelles and in liposomes. (b,d) - Distance distributions obtained by fitting data from (a, c) by MEM with background auto-correction.

539 in α-ddm micelles

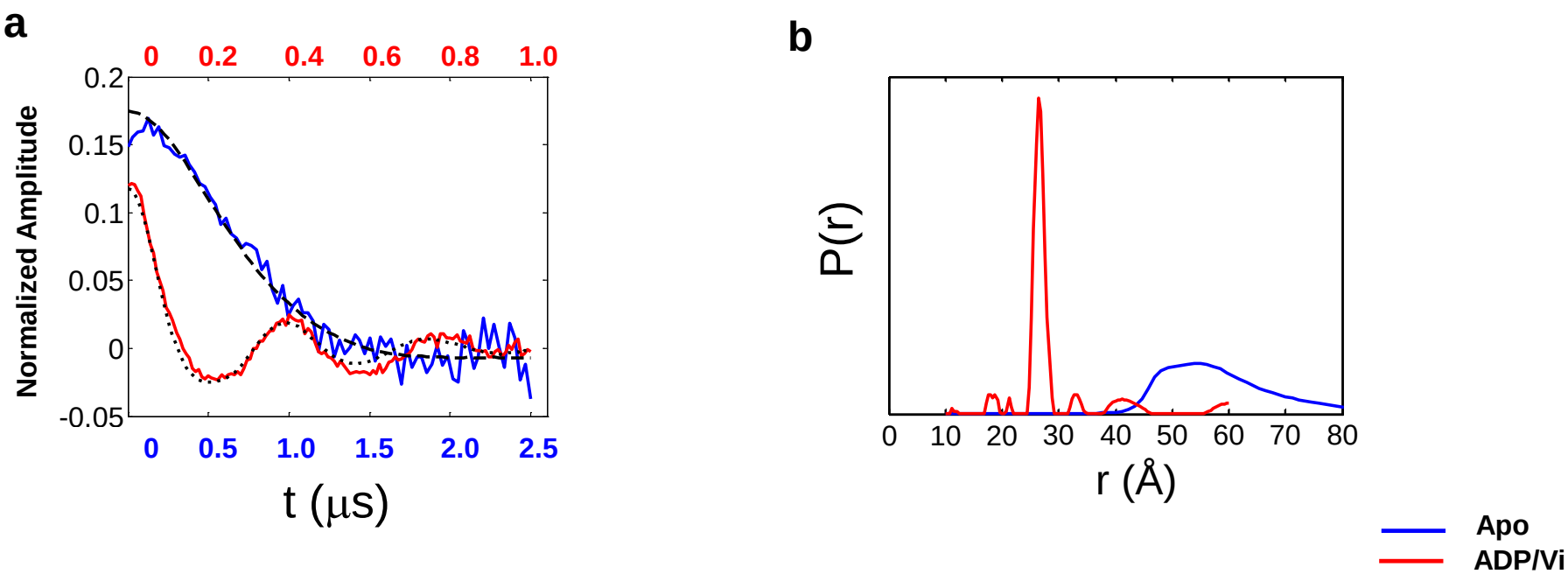

Supplementary Figure S4. (a) – Time domain 17.35 GHz DEER signals (after background removal) for MsbA mutant 539 in α-ddm for both apo and ADP/Vi states are shown together with their fits (dashed lines). (Different time-scales were used in plotting signals of apo and ADP/Vi intermediate). (b) – Distance distributions obtained in fitting data from (a) by MEM with background auto-correction.

103 in α-ddm micelles

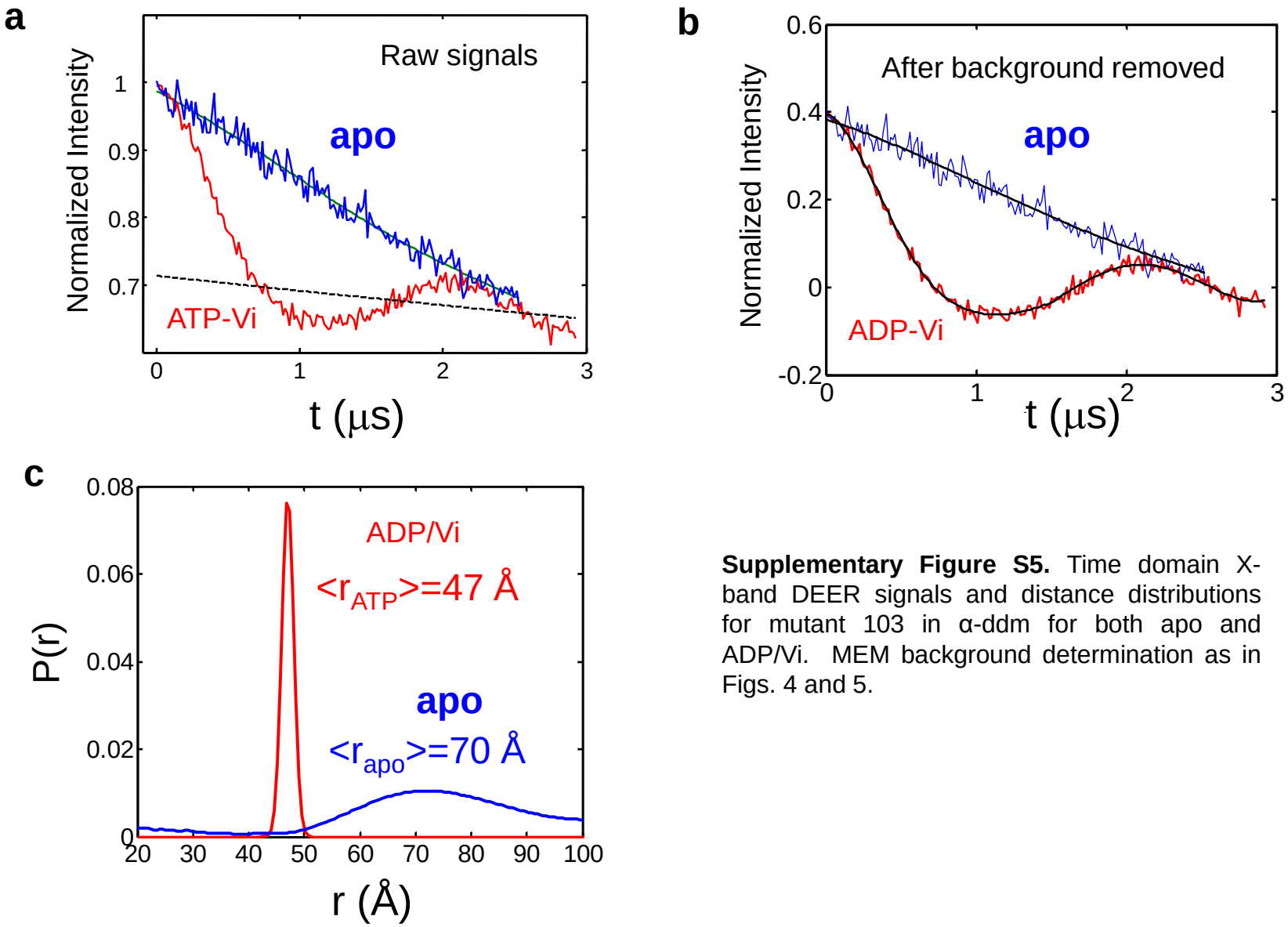

Supplementary Figure S5. Time domain X-band DEER signals and distance distributions for mutant 103 in α-ddm for both apo and ADP/Vi. MEM background determination as in Figs. 4 and 5.

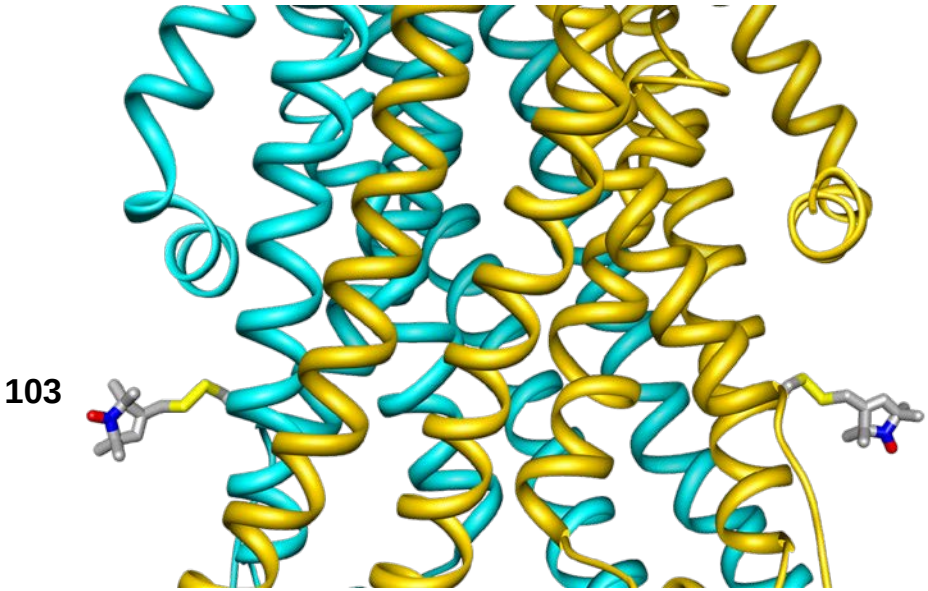

Supplementary Figure S6. Model of the spin label at site 99 of Sav1866 (equivalent to MsbA 103) shown on a ribbon representation of Sav1866.

LPS titration of MsbA

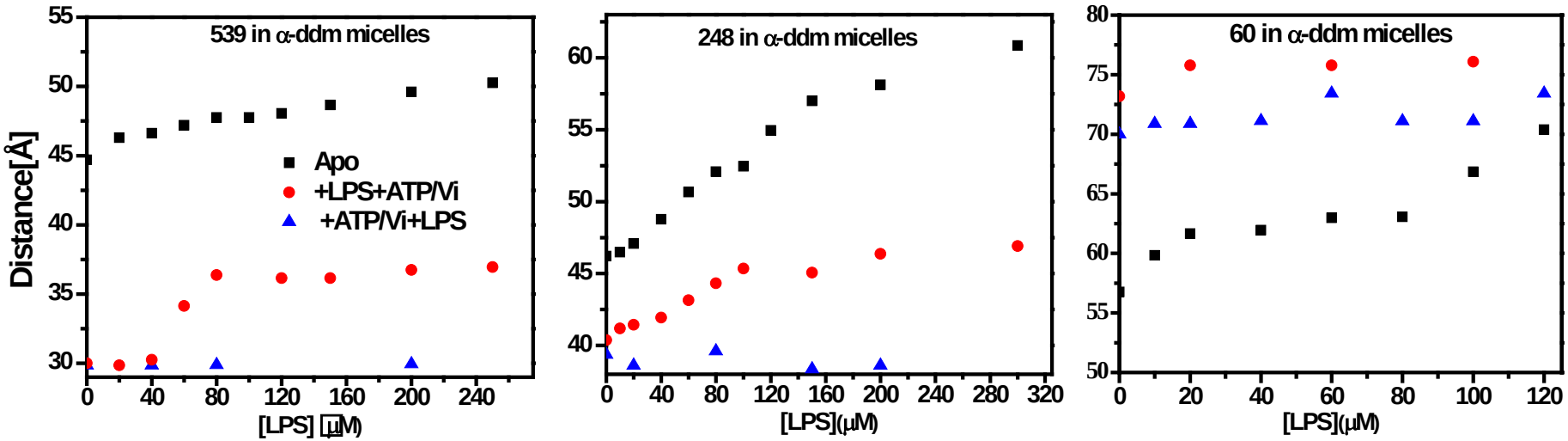

Supplementary Figure S7. Distance changes as a function of LPS concentration at three sites in MsbA . Distances were calculated from homotransfer between fluorescein probes as described in the materials and methods section. LPS increases monomer/monomer distances at all sites explored. The effects of LPS are inhibited by prior formation of the ADP/Vi intermediate.

61 in α-ddm micelles
Effects of LPS

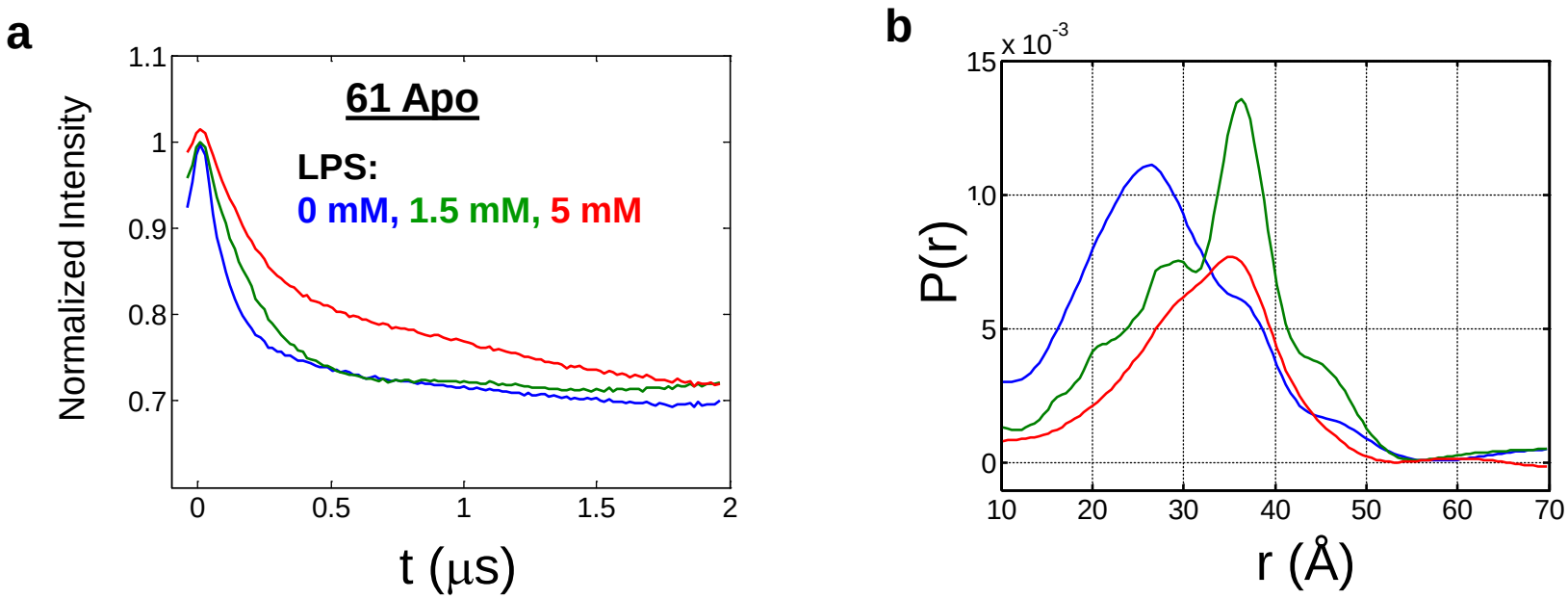

Supplementary Figure S8. (a) Raw 17.35GHz DEER signals and (b) distance distributions for spin labels introduced at site 61 in the presence of LPS.